EFFICIENT PROPULSION STRUCTURE WITH AN AXIAL FLUX ROTARY CONVERTER FOR HEV DRIVE UNIT

Ales HAVEL[1], Petr VACULIK[1], David SLIVKA[1]

[1]Department of Electronics, Faculty of Electrical Engineering and Computer Science, VSB - Technical University of Ostrava, 17. listopadu 15, Ostrava, 708 33, Czech Republic

ales.havel@vsb.cz, petr.vaculik@vsb.cz, david.slivka@vsb.cz

Abstract. *This paper describes an efficient axial flux arrangement of the four quadrant rotary converter for hybrid electric vehicles. The design of the axial flux wound stator and both axial flux squirrel cage rotors is based on the arrangement of radial air gap induction motor and permanent magnet synchronous motor. The method of constant magnetic circuit volume is utilized for dimensions conversion, which results into basic dimensions of stator and rotor discs in axial flux conception. This allows the creation of real 3D models in the CAD application. Finally, the finite element simulation of magnetic flux density and magnetic flux vector map in the area of axial flux stator pack are presented in the concluding part of this paper.*

Keywords

Axial flux machine, electromagnetic simulation, finite element method, hybrid electric vehicle, induction motor design, rotary converter, squirrel cage rotor, wound stator.

1. Introduction

The maximal efficiency of the internal combustion engine (ICE) used in conventional vehicles is due to Carnot's cycle approximately bounded above to 40 %. Such efficiency can only be reached in a very small torque-speed area, which leads to the idea of full torque and speed control in hybrid electric vehicle (HEV) conceptions aimed at considerable power savings. Many of today's used HEV conceptions are based on the series-parallel hybrid arrangement, combining together the advantages of both essential arrangements [1].

The main task of here presented four quadrant axial flux rotary converter (AFRC) is to keep the ICE working in the area of its maximal efficiency during all possible driving conditions to satisfy minimal fuel consumption. In other words, the AFRC have to convert the optimal torque-speed operation point of the ICE on the input shaft to the required variable torque and speed on the output shaft, which is through the final gear (FG) connected to the wheels.

The AFRC is supplied by the three phase voltage inverter (INV) from the DC power source, which can be realized as a combination of two autonomous power sources – LiFePO$_4$ battery pack delivering nominal current and ultracapacitor pack for peak power supplying.

Whole system is controlled by the DSP TMS320F28335 with implemented direct torque control algorithm to satisfy sufficient computing power and dynamics of the four quadrant rotary converter (4QRC) drive system – see Fig. 1 [2], [3], [4].

2. Axial Flux Rotary Converter

The proposed solution combines two known principles of electric rotating machines together in one unit, which is composed from synchronous and asynchronous machine having two rotors affixed to the input and output shaft, one wound stator and two axial air gaps δ_1 and δ_2. Due to selected double rotor arrangement it is possible to vary both the speed and the torque between the input and output shaft, hence the transferred power. The input and output power difference is possible to supply or consume by the stator winding, so only a part of the total vehicle drive energy is transferred across the electromagnetic coupling.

The unneeded part of mechanical energy produced by the ICE or the vehicle braking energy can be transferred through the electromagnetic coupling between the outer rotor and stator and then stored into the rechargeable batteries or ultracapacitor pack. On the other

hand, during the fluent change of the input and output shaft speed ratio it is possible to simultaneously

compensate the peak power consumption needed for dynamic states during speed variation or vehicle loading.
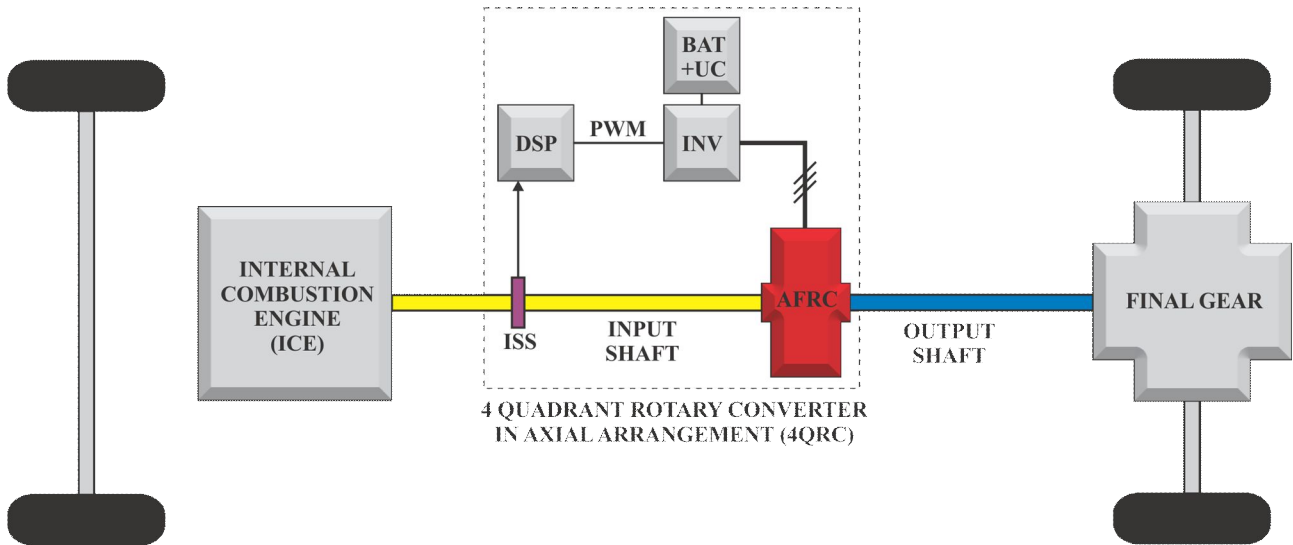
Fig. 1: Integration of the axial flux rotary converter into the HEV drive unit.

Constructional simplicity of presented axial flux rotary converter is ensured by the disc conception with two axial air gaps and double squirrel cage inner rotor. The inner rotor can simultaneously interact with electromagnetic fields from permanent magnet outer rotor and wound stator to create two different asynchronous machines with them – see Fig. 2.

the AFRC can be run in pure mechanical or electrical mode when only the ICE or batteries are producing the driving power.

3. Stator and Cage Rotor Design

The design of the axial flux stator and rotor is based on the design of standard worldwide used cylindrical conception of induction and synchronous motors. The resulting parameters are then recounted to the axial conception, more precisely, to the inner and outer diameters and thicknesses of the axial stator and rotor utilizing the method of constant magnetic circuit volume.

Fig. 2: The AFRC machine in axial cross section.

Another advantage of axial flux conception is in the possibility of air gap width adjustment, which allows the optimization of magnetic field depth penetration into the squirrel cage inner rotor. It also comes through that

The proportioning of the standard cylindrical motor usually starts with the determination of the machine diameters like stator diameter D_e, stator bore diameter D and the ideal air gap length l_i. The diameters D and l_i depend on the output motor power P_i, angular speed ω_S and electromagnetic loads A and B_δ. In the first stage of calculation, all the variables from (1) are unknown, except the synchronous angular speed, which is given by the optimal torque-speed operation point of the ICE, so the calculation is coming out from the recommended electromagnetic loads, coefficients α_δ, k_B, k_V and approximately determined electromagnetic power [5], [6].

$$\frac{D^2 l_i \omega_s}{P_i} = \frac{2}{\pi \alpha_\delta k_B k_V A B_\delta}. \qquad (1)$$

3.1. Axis Height and the Stator Diameter

The axis height $h = 80\,mm$ for the 1,5 kW 6 pole induction motor was chosen from the Fig. 1. Thereby the stator diameter D_e will be 131 mm, using the Tab. 1 as follows.

Tab.1: Axis heights accordant with the stator diameters.

h [mm]	56	63	71	80	90	100	112	132
D_e [m]	0,089	0,1	0,116	0,131	0,149	0,168	0,191	0,225
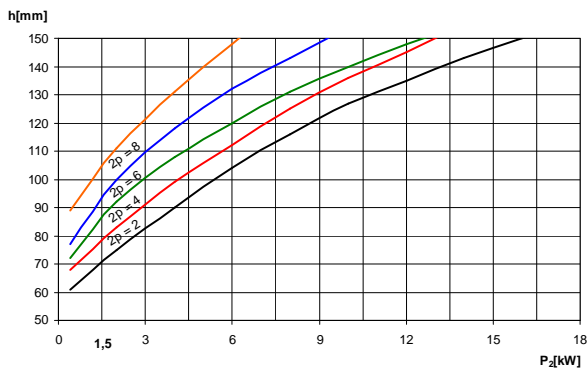
Fig. 3: Recommended axis heights of induction motor in dependency on its output power and number of poles.

3.2. The Stator Bore

Considering the same magnetic flux density in the particular parts of magnetic circuits in machines with the same stator bore, the height of the yoke will be directly proportional to the magnetic flux, thus inversely proportional to the pole number. If the slot diameters are independent on the number of poles, the stator bore can be approximately calculated using (2) [5].

$$D = k_D D_e = 0,71 \cdot 0,131 = 0,093m . \qquad (2)$$

Tab.2: The ratio $k_D = D/D_e$ for various pole numbers.

2p	2	4	6	8	10 - 12
k_D	0,52 – 0,57	0,62 – 0,68	0,70 – 0,72	0,74 – 0,75	0,75 – 0,77

3.3. Choice of the Electromagnetic Loads

While the induction motor diameters are inversely proportional on the product of linear current density A and magnetic flux density B_δ as mentioned before in (1), electromagnetic properties are affected by their mutual ratio. To calculate the ideal air gap length l_i, the magnetic flux density in the air gap (Fig. 4) and the linear current density (Fig. 5) have to be empirically predetermined from the graphs below, as in (3).

$$A = 22 \cdot 10^3\,Am^{-1} \quad B_\delta = 0,84T . \qquad (3)$$
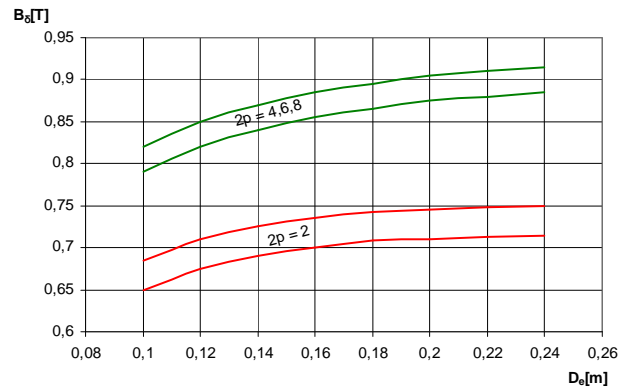
Fig. 4: The areas of optimal magnetic flux density in the air gap of induction motor in dependency of the stator diameter.
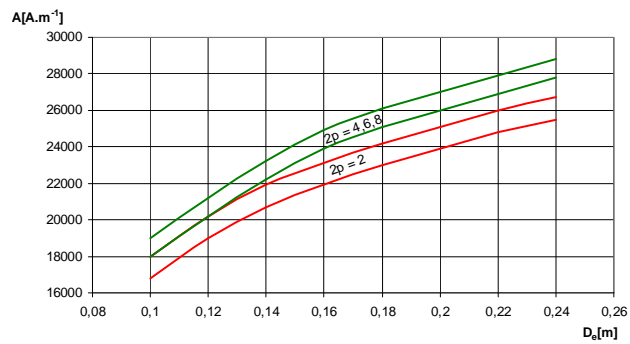
Fig. 5: The areas of optimal linear current density of induction motor in dependency of the stator diameter for various pole numbers.

3.4. Inner Motor Power

The last important parameter, which is necessary for the ideal air gap length calculation, is the inner motor power P_i. The coefficient k_E from (4) is the induced/rated voltage ratio. The optimal efficiency and power factor areas are possible to determine empirically from [5].

$$P_i = P_2 \frac{k_E}{\eta \cos \varphi} = 1500 \frac{0,94}{0,4 \cdot 0,73} = 2610VA . \qquad (4)$$

3.5. Ideal Air Gap Length and Thickness

Providing harmonic electromagnetic field in the air gap, the coefficients α_δ, k_B and k_V are chosen by default in (5):

$$\alpha_\delta = \frac{2}{\pi} \quad k_B = \frac{\pi}{2\sqrt{2}} \quad k_V = 0,95 . \qquad (5)$$

Since all the main electromechanical parameters are calculated or empirically predetermined, the ideal air gap length l_i can be simply expressed from (1).

$$l_i = \frac{2610 \cdot \sqrt{2} \cdot 60}{\pi^2 \cdot 0,093^2 \cdot 10^6 \cdot 0,95 \cdot 22 \cdot 0,84} = 0,148m \, . \quad (6)$$

The airgap size is calculated empirically using (7).

$$\delta \approx (0,25 + D) \cdot 10^{-3} = (0,25 + 0,093) \cdot 10^{-3} = 0,35mm \, . (7)$$

3.6. The Rotor Diameters

Considering the radial conception of IM, the outer diameter of the rotor is given by the stator bore diameter lowered by 2δ, as in (8).

$$D_2 = D - 2\delta = 0,093 - 2 \cdot 0,35 \cdot 10^{-3} = 0,029m \, . \quad (8)$$

The rotor package is in most cases put on the shaft directly, so the inner diameter of the rotor equals to the shaft diameter and is given by the size of the coefficient k_i as presented in (9).

$$D_i = k_i D_e = 0,44 \cdot 0,131 = 0,058m \, . \quad (9)$$

3.7. Electromagnetic Parameters

To calculate the electromagnetic parameters of the induction motor, the number and type of stator and rotor slots have to be specified. The number of stator slots Q_1 must be dividable by the number of phases and the number q, which is the count of slots per pole and phase and should be an integer. The number of rotor slots Q_2 is chosen from the recommended range for 6 pole motors.

$$Q_1 = 36, \quad Q_2 = 42 \quad q = \frac{Q_1}{2pm} = \frac{36}{2 \cdot 3 \cdot 3} = 2 \, . \quad (10)$$

The stator nominal current:

$$I_{1N} = \frac{P_2}{mU_N \eta \cos\varphi} = \frac{1500}{3 \cdot 231 \cdot 0,74 \cdot 0,73} = 4A \, . \quad (11)$$

The number of effective conductors in the slot:

$$V_d = \frac{\pi D A}{I_{1N} Q_1} = \frac{\pi \cdot 0,093 \cdot 22000}{4 \cdot 36} = 45 \, . \quad (12)$$

The number of coils:

$$N_1 = \frac{V_d Q_1}{2m} = \frac{45 \cdot 36}{2 \cdot 3} = 270 \, . \quad (13)$$

After the specification of the nominal motor current and the number of coils it is important to recalculate the values of electromagnetic loads again and verify if they are still in the allowed range.

The linear current density:

$$A = \frac{2I_{1N}N_1 m}{\pi D} = \frac{2 \cdot 4 \cdot 270 \cdot 3}{\pi \cdot 0,093} = 22179 Am^{-1} \, . \quad (14)$$

The magnetic flux:

$$\Phi = \frac{k_E U_{1N}}{4k_B N_1 k_V f_1} = \frac{0,94 \cdot 231 \cdot 2\sqrt{2}}{4\pi \cdot 270 \cdot 0,95 \cdot 50} = 3,8 \cdot 10^{-3} Wb \, . (15)$$

The magnetic flux density in the air gap:

$$B_\delta = \frac{p\Phi}{Dl_i} = \frac{3 \cdot 3,8 \cdot 10^{-3}}{0,093 \cdot 0,148} = 0,83T \, . \quad (16)$$

4. Conversion to Axial Conception

As mentioned above, the cylindrical stator and rotor dimensions including the ideal air gap length have to be converted into the axial flux conception using the method of the constant magnetic circuit volume. It is also obvious that the inner and outer disc diameters should be the same for disc stator and disc rotor. The stator and rotor volume equations (17) and (18) are presented below.

$$\frac{\pi \cdot l_i}{4}\left[D_e^2 - D^2\right] = \frac{\pi h_S}{4}\left[D_{OUT}^2 - D_{IN}^2\right], \quad (17)$$

$$\frac{\pi \cdot l_i}{4}\left[D_2^2 - D_i^2\right] = \frac{\pi h_R}{4}\left[D_{OUT}^2 - D_{IN}^2\right], \quad (18)$$

where are:

- h_S and h_R the disc stator/rotor thicknesses,

- D_{IN} and D_{OUT} inner /outer disc diameters.

By the comparison of the equations (17) and (18) is possible to express the stator/rotor disc thicknesses ratio (19) and the outer disc diameter dependency (20), which finally leads to all main dimensions of the axial flux stator and rotor in (21).

$$\frac{h_S}{h_R} = \frac{D_e^2 - D^2}{D_2^2 - D_i^2} = \frac{0,131^2 - 0,093^2}{0,092^2 - 0,058^2} = 1,67 \, . \quad (19)$$

$$D_{OUT} = \sqrt{\frac{0,148 \cdot \left(0,131^2 - 0,093^2\right)}{0,050} + 0,08^2} = 0,178m \, . (20)$$

$$\begin{array}{ll} h_S = 0,050m & D_{IN} = 0,080m \\ h_R = 0,030m & D_{OUT} = 0,178m \end{array} \quad (21)$$

The right choice of the air gap thicknesses δ_1 and δ_2 has crucial influence on the energetic parameters of the AFRC drive unit. If the size of the air gap is reduced, also the magnetizing current decreases, which leads to better power factor and lower stator losses. However, making the air gap too thin may cause increasing of the amplitude of magnetic flux density pulses in the air gap, hence increasing the surface and pulse losses [5], [7].

Therefore the optimal air gap thickness has to be evaluated as a result of the 3D finite element method simulations.

4.1. Comparison with the Fabricated Motor

The comparison has been made with the 6 pole axial flux induction motor fabricated by the British corporation Brook Crompton [8].

Tab.3: Comparison between the Designed and Fabricated IM.

	Designed motor	Fabricated axial flux IM
2p [-]	6	6
P_2[W]	1500	1500
U_{IN}[V]	400	400
I_{IN}[A]	4	4,2
f_{IN}[Hz]	50	50
h_S[mm]	50	50
h_R[mm]	30	29
D_{IN}[mm]	80	80
D_{OUT}[mm]	178	180

5. 3D Models

The 3D models of disc stator and rotor situated below are created in the CAD application Autodesk Inventor Professional. The geometry is then transported to the modern finite element (FEM) environments and solvers like Ansoft Maxwell or Ansoft RMxprt, towards running the magnetostatic, electromagnetic and thermal simulations. The output data could be fundamental for further design and optimization of the drive units utilizing the axial flux motors as a main or auxiliary drive.
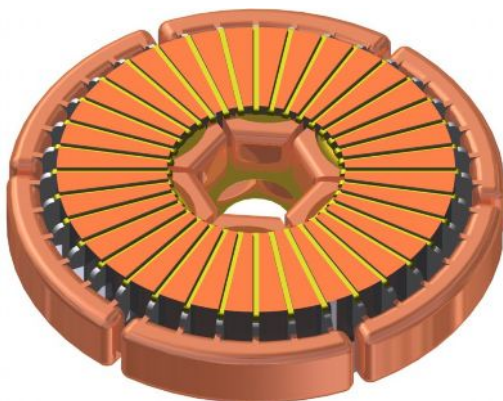
Fig. 6: The 3D model of an axial flux stator with stranded winding.
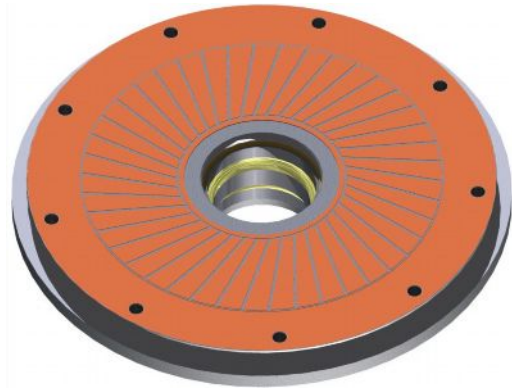
Fig. 7: The 3D model of an axial flux squirrel cage rotor.

Fig. 8: The 3D model of stator housing.

6. 3D FEM Simulations

Ansoft Maxwell is specialized software usually used for the simulations of electromagnetic fields during the design and analysis of the electric motors, transformers, drives and other electromechanical machines intended for automobile, army or aircraft industry. It is based on the FEM method and allows accurate 2D and 3D simulations in time and frequency domains.

6.1. Axial Flux Stator Analysis

The relatively easy handling of Maxwell application is demonstrated on the creation and parameterization of the 3D geometry of the 6 pole axial flux stator model with two layer winding. The winding parameterization was started after the slot shape specification, which is shown on the figures below. After setting the boundary conditions and excitations, it is possible to start the mesh creation and run the simulations of the magnetic flux density and vector map of magnetic flux distribution around the structure of the stator pack. The results are

shown on the Fig. 11. and Fig. 12.
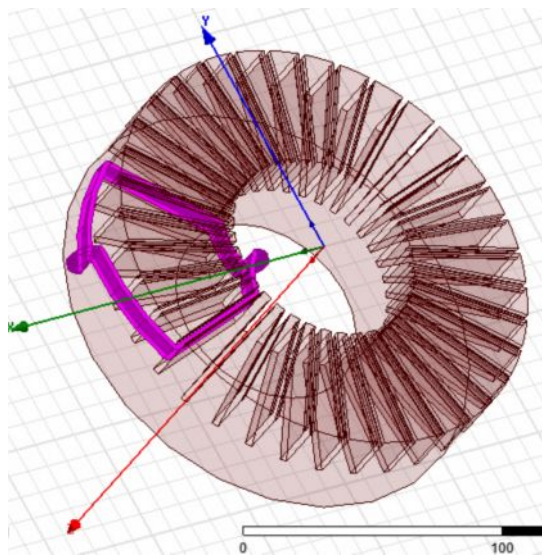
Fig. 9: The creation of one stator coil for six pole stator.

Fig. 10: The parameterization of the stator pack in Maxwell.
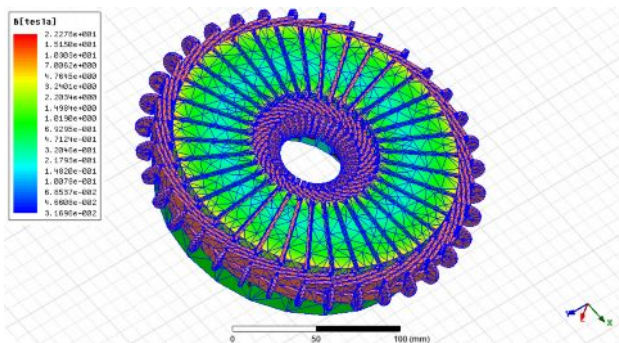
Fig. 11: The distribution of magnetic flux density on the surface of the stator pack with indicated mesh.
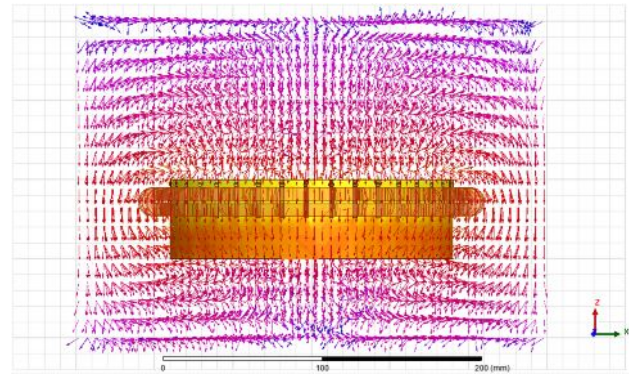
Fig. 12: The vector map of magnetic flux density around the stator pack.

7. Conclusion

This paper has proven that the old approach of cylindrical induction motor design is also applicable for designing the axial flux motors with great accuracy. The simulation results are in accordance with the predetermined and calculated values of the magnetic flux density presented in (3) and (16).

Axial air gap motors may one day became a key candidate for propulsion systems of hybrid or pure electric vehicles. To utilize this technology in practical applications, the 3D finite element analysis is needed for better understanding of electromagnetic conditions such as flux and field behaviors in drive structures involving the axial flux based machines.

Acknowledgements

References

[1]   LARMINIE, J., LOWRY, J. *Electric Vehicle Technology Explained*. John Wiley & Sons, Ltd, 2003, England, pp. 296, ISBN 0-470-85163-5.

[2]   CHLEBIS, P., DUDEK, J. Comparison of Power Losses and Quality of Output Voltage from Different Types of Inverters. In: *35th Annual IEEE Power Electronics Specialists Conference*, Aachen, Germany, 2004, Vol. 1-6, pp. 3120-3126, ISBN 0-7803-8399-0.

[3]   BRANDSTETTER P., CHLEBIS P., PALACKY P. Direct Torque Control of Induction Motor with Direct Calculation of Voltage Vector. *Advances in Electrical and Computer*

Engineering, vol. 10, n. 4, pp. 17-22, 2010, ISSN 1582-7445.

[4] CHLEBIS, P., HAVEL, A., VACULIK, P., PFOF, Z. Modern Instruments for increasing the Efficiency of the Energy Transfer in Electric Vehicles. In *14th EPE-PEMC 2010 International Power Electronics and Motion Control Conference*, September 6-8, Ohrid, Republic of Macedonia 2010, vol. 14., p. 89-93, ISBN 978-1-4244-7854-5.

[5] KOPYLOV I. P. and collective. *Construction of electric machines*. First release, Praha: SNTL, 1988, 688 p.

[6] GIERAS J., WANG R., KAMPER M. *Axial flux permanent magnet brushless machines*. Kluwer academic publisher 2004. ISBN 1-4020-2661-7.

[7] CHLEBIS, P., HAVEL, A., VACULIK, P., ODLEVAK L. The Design and Simulation of the Axial Air Gap Induction Motor. In *12th Electric Power Engineering 2011*, May 17-19, Kouty nad Desnou, Czech Republic, ISBN 978-80-248-2393-5.

[8] *Brook Crompton* [online]. 2011 [cit. 2011-09-09]. Axial airgap motors. Available at WWW: < http://brookcrompton.com/pdf-files/2701E%20Axial_web.pdf>.

About Authors

Ales HAVEL was born in Celadna in 1984. He obtained his Master's degree in field of power electronics systems and electric machines design in 2009. He is currently pursuing Ph.D. study at Department of Electronics at VSB-TU Ostrava on Faculty of Electrical Engineering and Computer Science. His research includes power systems, design and modeling of electric machines.

Petr VACULIK was born in Zlin in 1983. He received his Master's degree in field of Power Electronics Systems in 2007. He obtained his Ph.D. degree in Power converters and simulation of electric vehicles. Currently he acts at Department of Electronics at VSB-TU Ostrava on Faculty of Electrical Engineering and Computer Science.

David SLIVKA was born in Frydek in 1985. He received his Master's degree in field of drive control in 2009. He is currently pursuing Ph.D. study at Department of Electronics at VSB-TU Ostrava on Faculty of Electrical Engineering and Computer Science. His research includes drives control in electric vehicles.